

Supplementary Material for:

Targeting tumor-resident mast cells for effective anti-melanoma immune responses

Susanne Kaesler, Florian Wölbing, Wolfgang Eberhard Kempf, Yuliya Skabytska, Martin Köberle, Thomas Volz, Tobias Sinnberg, Teresa Amaral, Sigrid Möckel, Amir Yazdi, Gisela Metzler, Martin Schaller, Karin Hartmann, Benjamin Weide, Claus Garbe, Hans-Georg Rammensee, Martin Röcken and Tilo Biedermann

Figure S1

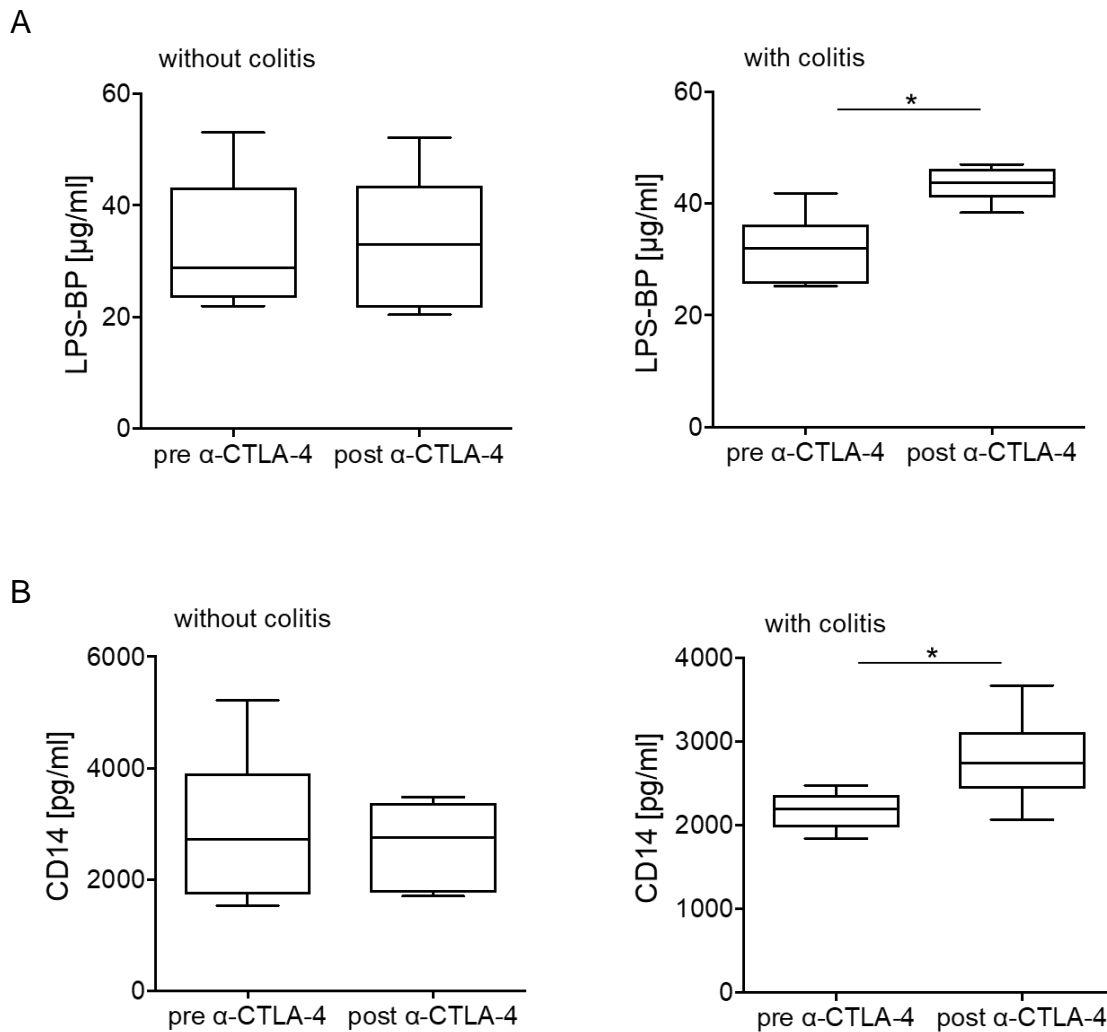


Figure S1: LPS-signature in melanoma patients with ipilimumab-induced colitis.

Analyses of serum samples before and after α -CTLA-4 treatment of stage IV melanoma patients as described in Fig. 1A. Serum levels of the LPS-inducible proteins LPS-BP (A) and sCD14 (B) as determined by quantitative ELISA are shown. Data are presented as the mean \pm SD and analyzed with the Wilcoxon test ($n = 6$ per group). * $p < 0.05$.

Figure S2

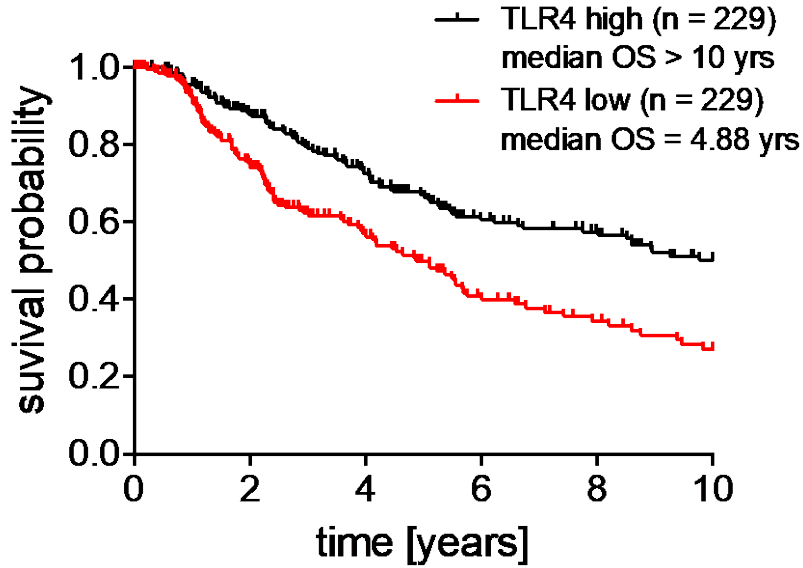
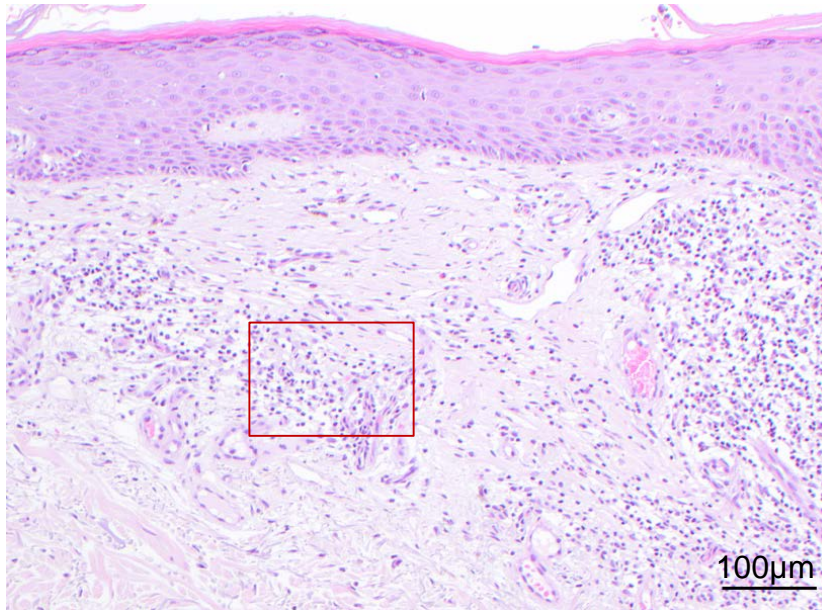


Figure S2: Prolonged survival of melanoma patients with high TLR4 expression

Kaplan-Meier analyses of The Cancer Genome Atlas (TCGA) dataset of 458 melanoma patients with high (black curve) and low (red curve) TLR4 levels based on the 50th percentile of gene expression showed significantly better patient survival in patients with high TLR4 levels. Statistical analysis was done with log-rank test using R software.

Figure S3

A



B

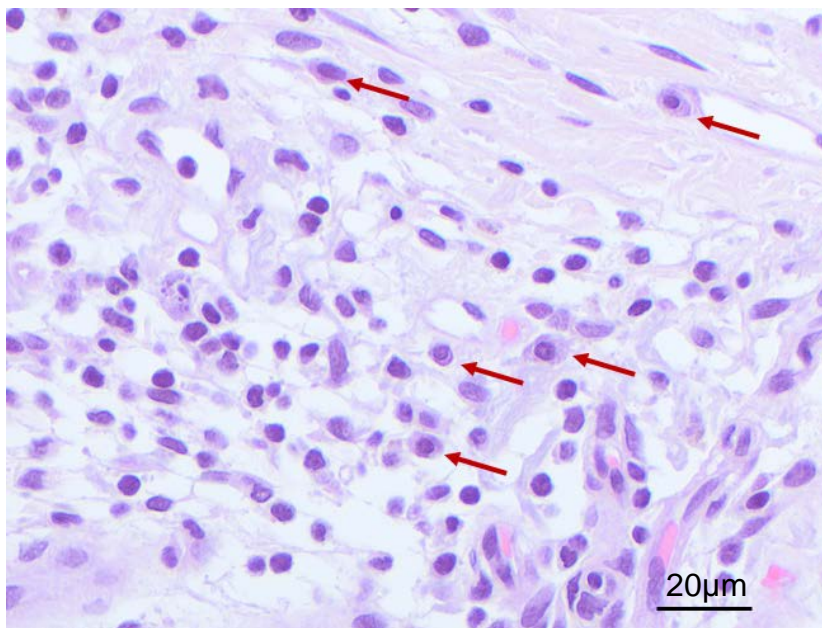


Figure S3: Accumulation of morphological MC-like cells in human melanoma with immune regression

Photomicrograph of H & E stained histological section from human melanoma with immune regression (A) and magnification thereof (B) as indicated by the red rectangle. (B) Red arrows label cells with morphology characteristic for MC.

Figure S4

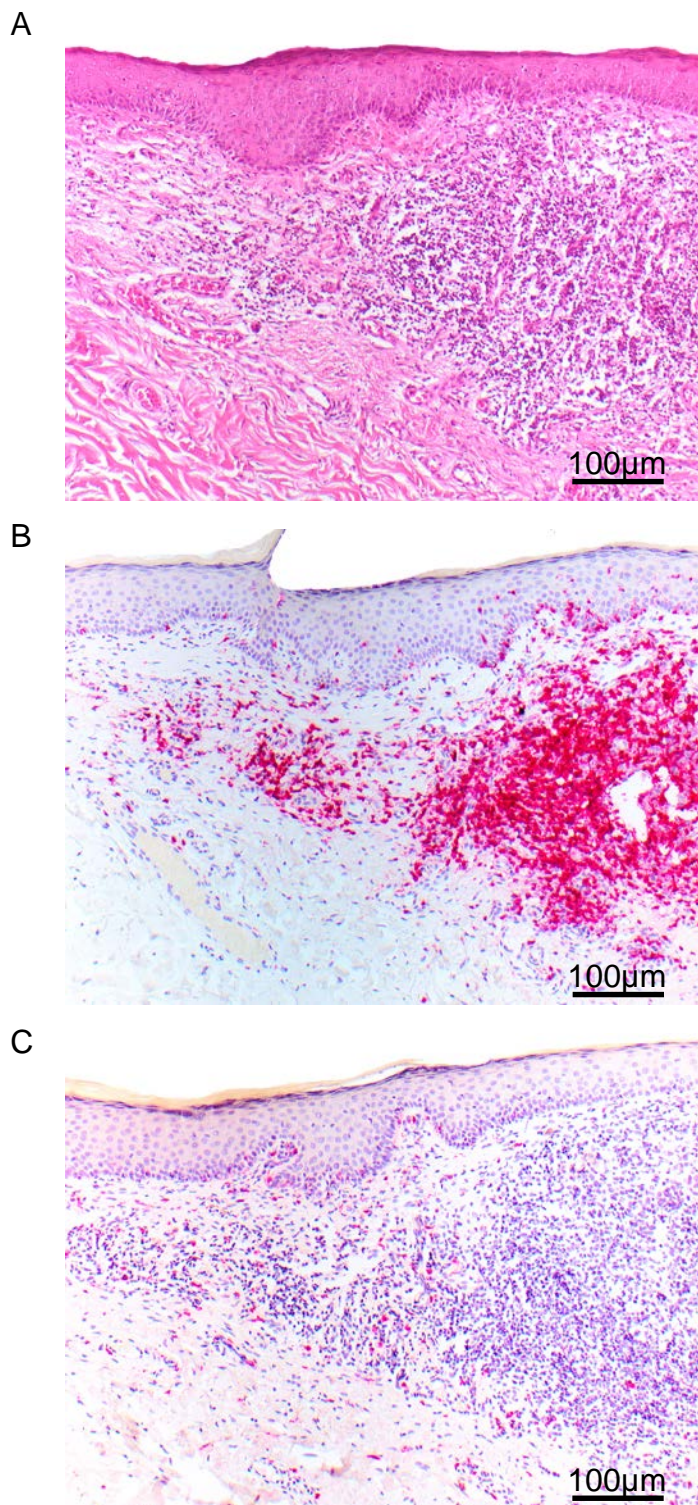


Figure S4: Strong infiltration of CD3⁺ lymphocytes in human melanoma with immune regression

Photomicrograph of (A) H & E stained histological section from the same human melanoma with immune regression shown in Figure 3A and Figure S3. (B, C) Immunohistochemistry with anti-CD3 staining T cells (B, red dye) and anti-tryptase staining MC (C, red dye) confirming a strong infiltration of T cells co-localizing with MCs within the regression area of the melanoma.

Figure S5

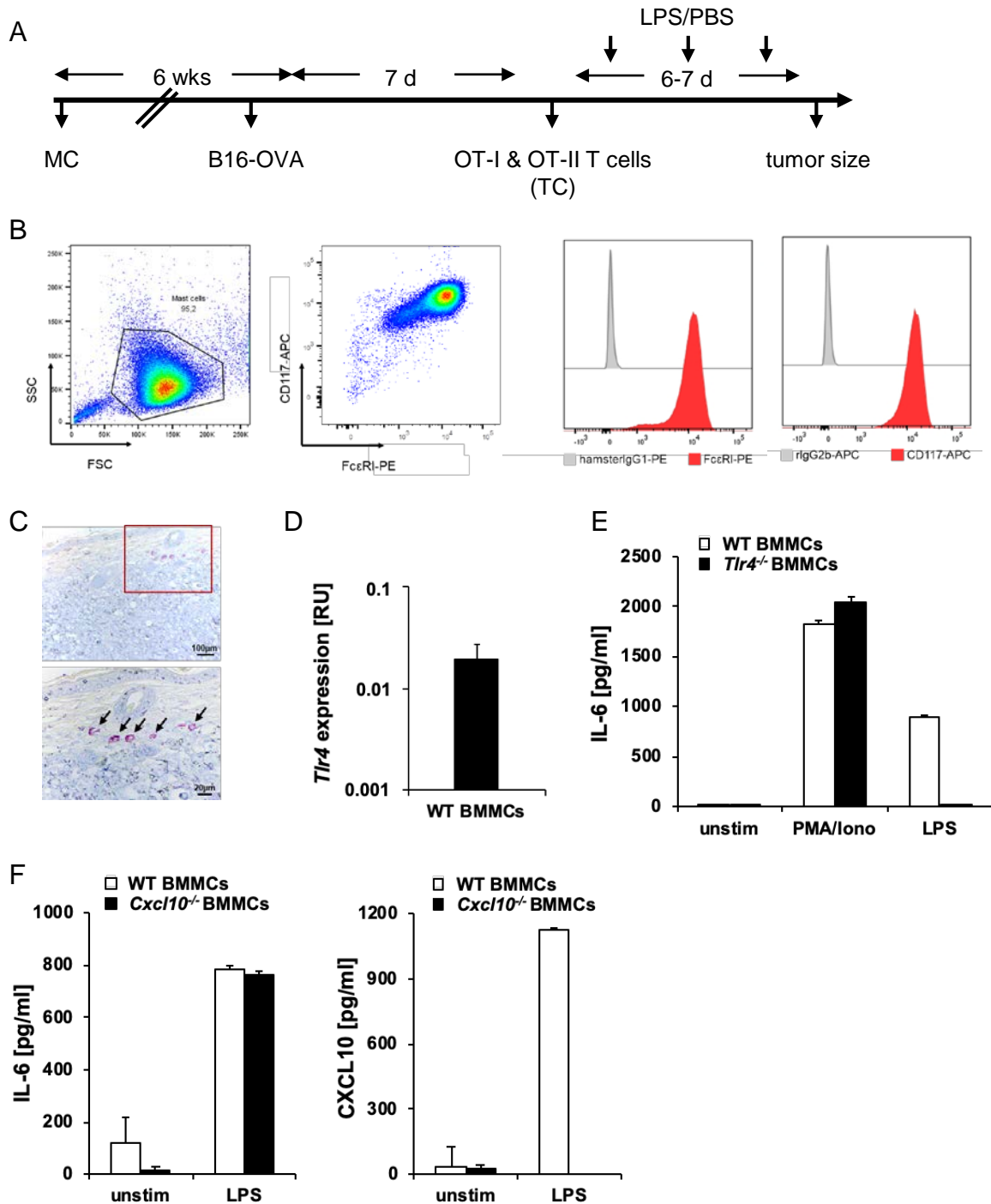


Figure S5: Characterization of BMMCs used for reconstitution of the skin with MCs

(A) Diagram of the mouse melanoma protocol including MC reconstitution six weeks prior to tumor cell implantation. (B) Representative flow cytometry analysis of bone marrow-derived mast cells (BMMCs) after 3 weeks of culture in conditioned medium. Mature BMMCs are characterized by high expression of FcεRI and CD117 depicted as dot blot (right) and as red histograms (left). For comparison isotype stainings (grey histograms) are shown. (C) Representative example of toluidin stained melanoma section from a MC-deficient mouse with MC-reconstitution before B16-OVA injection (top) and magnification from it (bottom), black arrows mark MCs. (D) *Tlr4* expression by WT BMMCs as determined by real-time PCR analysis. (E) IL-6 ELISA with supernatants from differentially stimulated WT and *Tlr4*^{-/-} BMMCs. (F) IL-6 and CXCL10 released from WT and *Cxcl10*^{-/-} BMMCs as determined by quantitative ELISA.

Figure S6

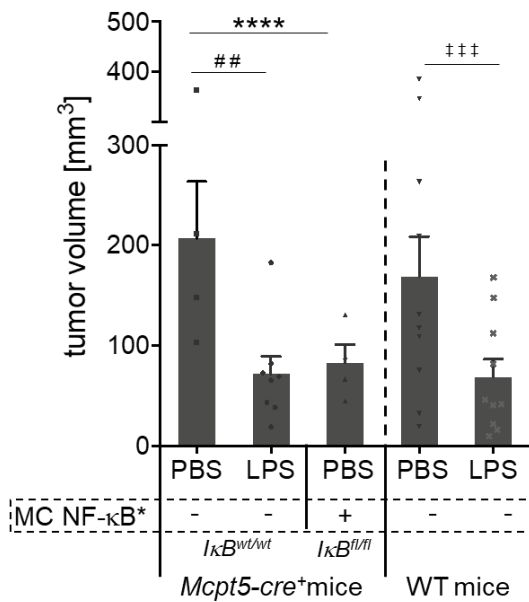


Figure S6: Melanoma immune control in *Mcpt5-cre*⁺ mice

Tumor volume [mm³] at the endpoint of the experimental protocol shown in Fig. 2A demonstrating LPS-induced tumor immune control in *Mcpt5-cre*⁺ *IκB*^{wt/wt} mice (left side) equivalent to PBS-treated *Mcpt5-cre*⁺ *IκB*^{fl/fl} mice with endogenously activated NF-κB in MC (MC NF-κB*) and to LPS-treated C57BL/6 WT mice (right side). Tumor volume in PBS-treated *Mcpt5-cre*⁺ *IκB*^{wt/wt} mice is comparable to that in PBS-treated WT mice (first bar on left and right side) (n = 4-10 per group; see also Fig. 2h). Means ± SEM are shown. p-values were calculated with 2-way ANOVA and Tukey's test; ## p < 0.005; ††† p < 0.0005; **** p < 0.0001

Figure S7

A

	1/2	3/4	5/6	7/8	9/10	11/12	13/14	15/16	17/18	19/20	21/22	23/24
A	reference											reference
B	CXCL13	C5/C5a	G-CSF	GM-CSF	CCL1	CCL11	sICAM-1	IFN-g	IL-1a	IL-1b	IL-1ra	IL-2
C	IL-3	IL-4	IL-5	IL-6	IL-7	IL-10	IL-13	IL-12p70	IL-16	IL-17	IL-23	IL-27
D	CXCL10	CXCL11	CXCL1	M-CSF	CCL2	CCL12	CXCL9	CCL3	CCL4	CXCL2	CCL5	CXCL12

B

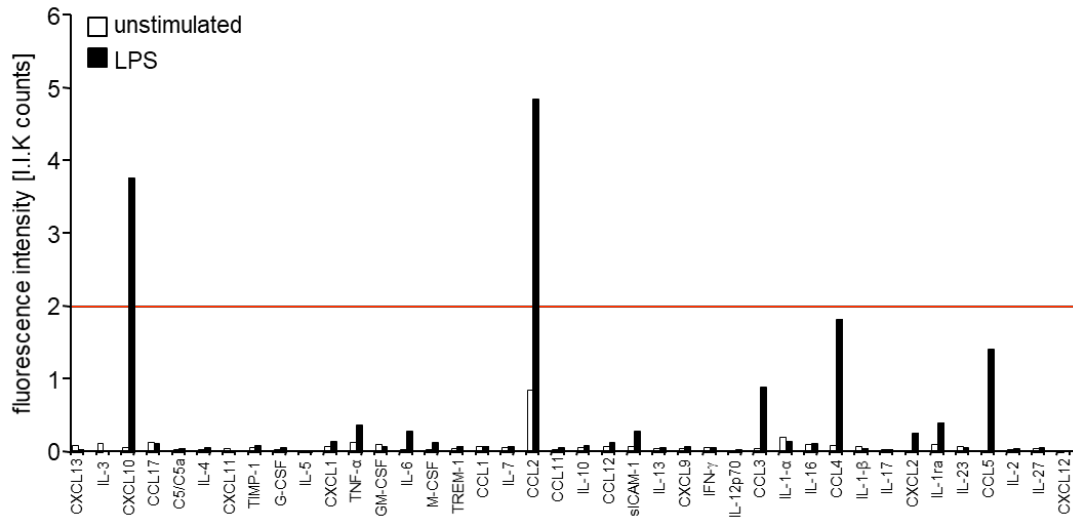


Figure S7: Cytokine profile of LPS exposed BMDCs

(A) Table of the cytokine antibodies and controls on the array blots shown in Fig 5A. (B) Densitometric quantification of the signals after incubation with supernatants from unstimulated or LPS-exposed BMDCs.

Figure S8

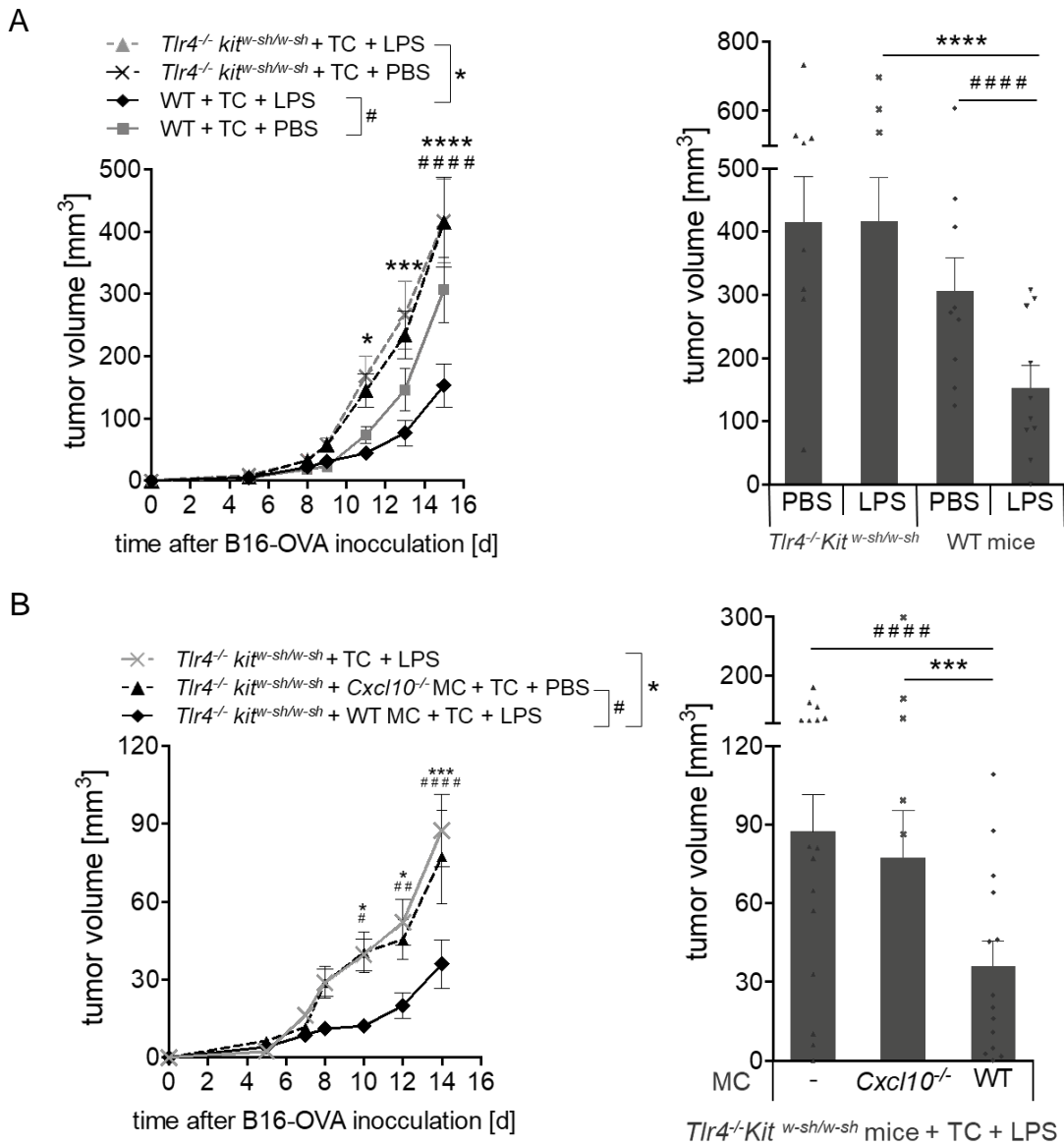


Figure S8: Melanoma immune control in *Tlr4*^{-/-} *Kit*^{W-sh/W-sh} mice

Tumor volume [mm³] over time (left) and at the endpoint of the experiment (right) according to the protocol shown in Fig. 2A. (A) *Tlr4*^{-/-} *Kit*^{W-sh/W-sh} mice deficient in both MC and TLR4 fail to establish LPS-mediated tumor immune defense in contrast with WT C57BL/6 mice (n = 8-10 per group). (B) Reconstitution of *Tlr4*^{-/-} *Kit*^{W-sh/W-sh} mice with WT but not with *Cxcl10*^{-/-} MCs resulted in LPS-induced effective tumor immune control (n = 14-16 per group). Data are presented as the mean ± SEM. p-values were calculated with 2-way ANOVA and Tukey's test; *, # p < 0.05; **, ## p < 0.005; ***, ###, ††† p < 0.0005; ****, ##### p < 0.0001.

Figure S9

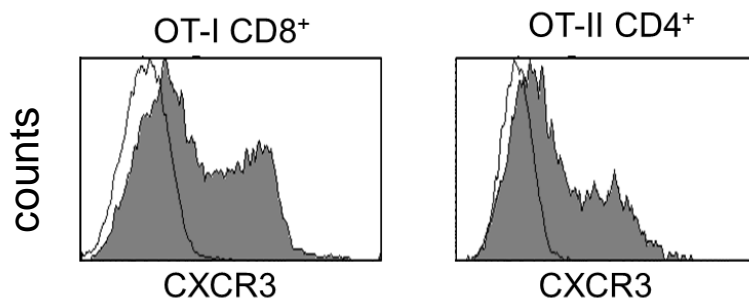


Figure S9: Tumor-specific OT-I and OT-II T cells express the CXCL10 receptor CXCR3

Tumor-specific OT-I (left) and OT-II (right) cells were analyzed for the expression of the CXCL10 receptor CXCR3 immediately before the adoptive transfer by flow cytometry. Representative examples of CXCR3 staining as filled histograms and isotype controls as open histograms.

Figure S10

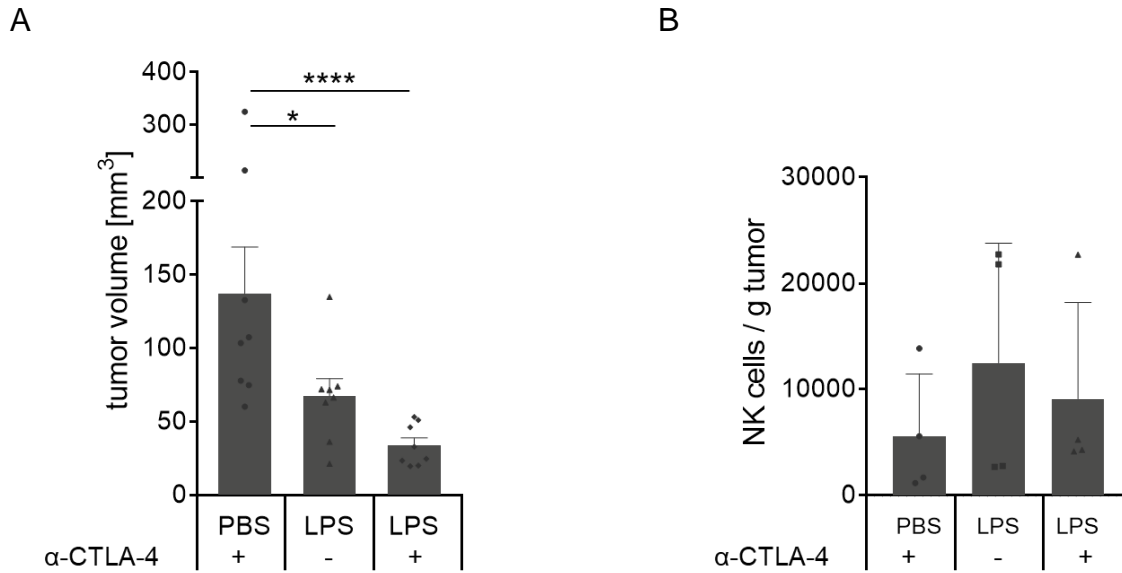


Figure S10: Flow cytometry analysis of different immune cells in melanoma.

WT C57BL/6 mice were treated according to the protocol shown in Figure 2A with additional application of α -CTLA-4 antibodies. (A) The tumor volume at the endpoint day14) (n = 8 per group). (B) Flow cytometry analysis of some melanomas from the experiment shown in (A) and Fig. 6B-D: NK-cells, determined as CD45⁺NK1.1⁺CD49b⁺ cells. (n = 3 per group). p-values were calculated with one-way ANOVA followed by Tukey's test. Means \pm SEM are shown.

Figure S11

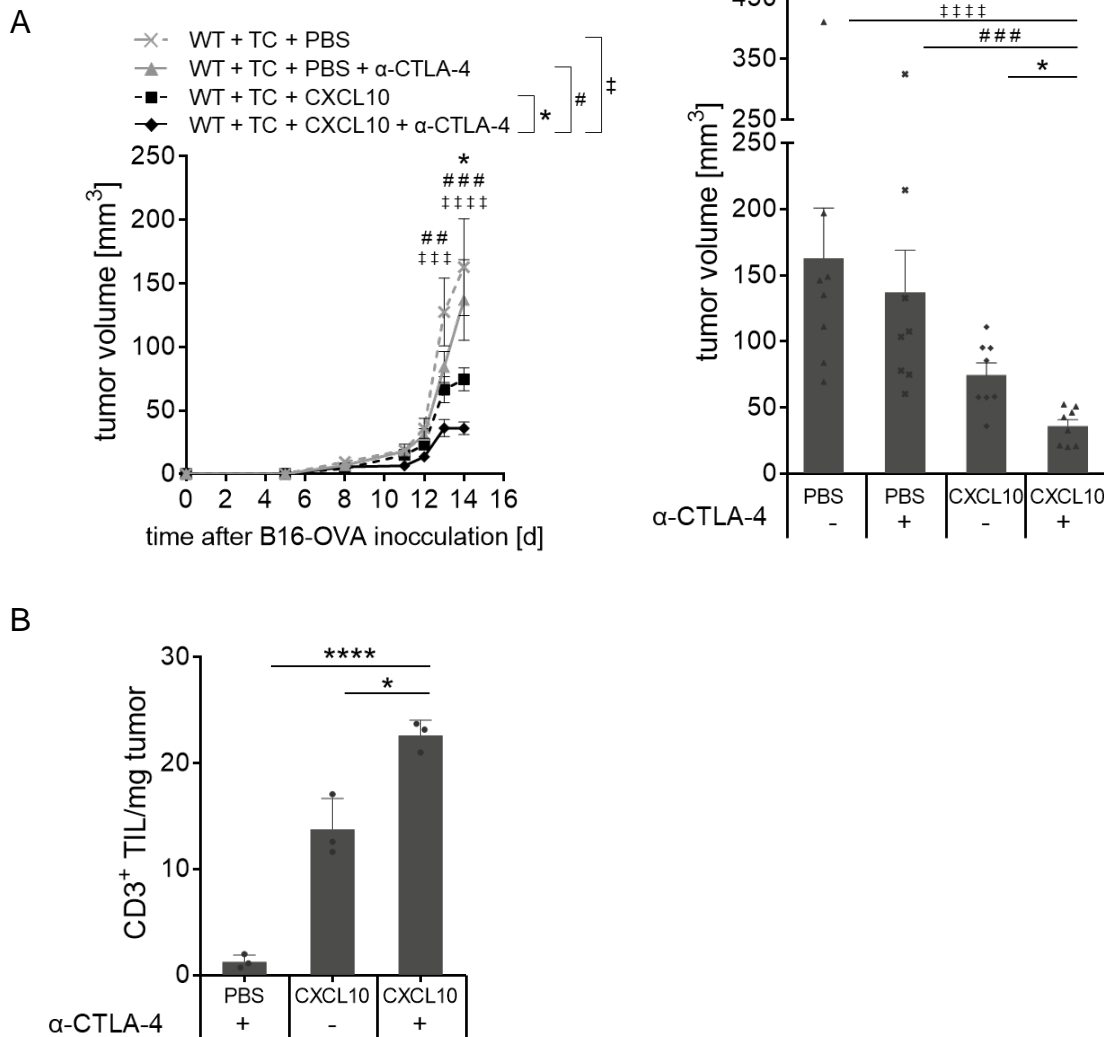


Figure S11: Immune checkpoint inhibitor treatment and complementation with LPS orchestrate effective melanoma immune defense

(A) The protocol shown in Figure 2a was extended by additional application of α -CTLA-4 antibodies. The tumor volume in WT C57BL/6 mice over time (left) and as bars at the endpoint (right) ($n = 8$ per group). (B) TILs as determined by flow cytometry analysis in melanomas from WT C57BL/6 mice ($n = 3$ per group). P-values were calculated with 2-way ANOVA (A) or with one-way ANOVA (B) followed by Tukey's test. Means \pm SEM (A) or Means \pm STDev (B) are shown.